8.3 MONITORING OF TOTAL FLUX USING A KSP TYPE VIDEO CONVERTER

By

Kouichi SEBATA, Jun AMAGAI, Tetsuro KONDO,
and Noriyuki KURIHARA

ABSTRACT

In the Keystone project (KSP) Very Long Baseline Interferometer (VLBI) system, there is a power monitor in the video converter. Using this monitor we can measure interference and system noise increases caused by obstacles located around the antenna. Using this monitor we can also derive the correlated fluxes of radio sources from the correlation amplitude observed by VLBI. Here we introduce this power monitor system with some application results.

Keywords: VLBI, KSP, Power monitor, System noise

1. Introduction

In a conventional geodetic VLBI technique, many frequency channels in an IF band signal are converted into video-frequency-band signals ranging from 0 to several MHz. They are utilized for a bandwidth synthesis in order to accurately determine the observed delay[1]. A video converter converts IF signals into video signals[2]. The video converter uses an image rejection mixer to obtain an upper side band and lower side band signal and an input interface unit finally converts video signals into digital signals[2]. Since the input interface has a range of input signal levels, these need to be adjusted in order for the unit to work properly. Therefore the video converter is equipped with an output level monitor that can calibrate the correlation amplitude of radio sources. In this paper, we will describe this calibration method by using the readout of video-converter-output level and results obtained from the observation data.

2. Occurrence of Interferences at Each Station

The readout of the video-converter-output monitor can be used to monitor the occurrence of interferences and to survey the direction of interferences at each station. Figs. 1 and 2 show examples of interference surveying
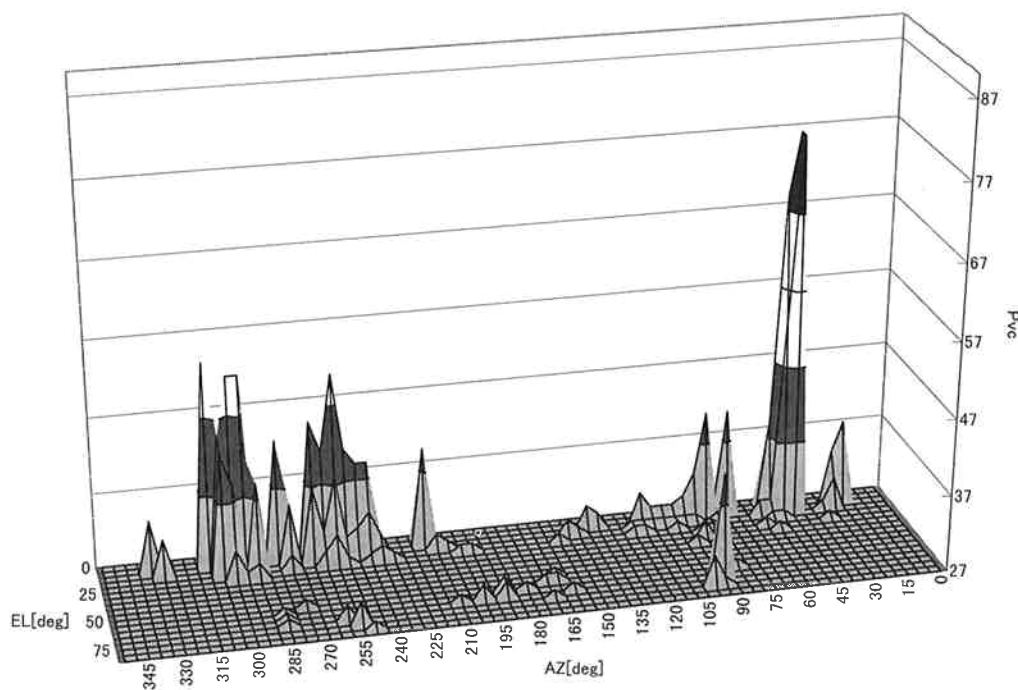

Fig. 1   Result of interference surveying made at Koganei (2ch USB, Aug.22/1998). Pvc is the readout of video-convertor-monitor.
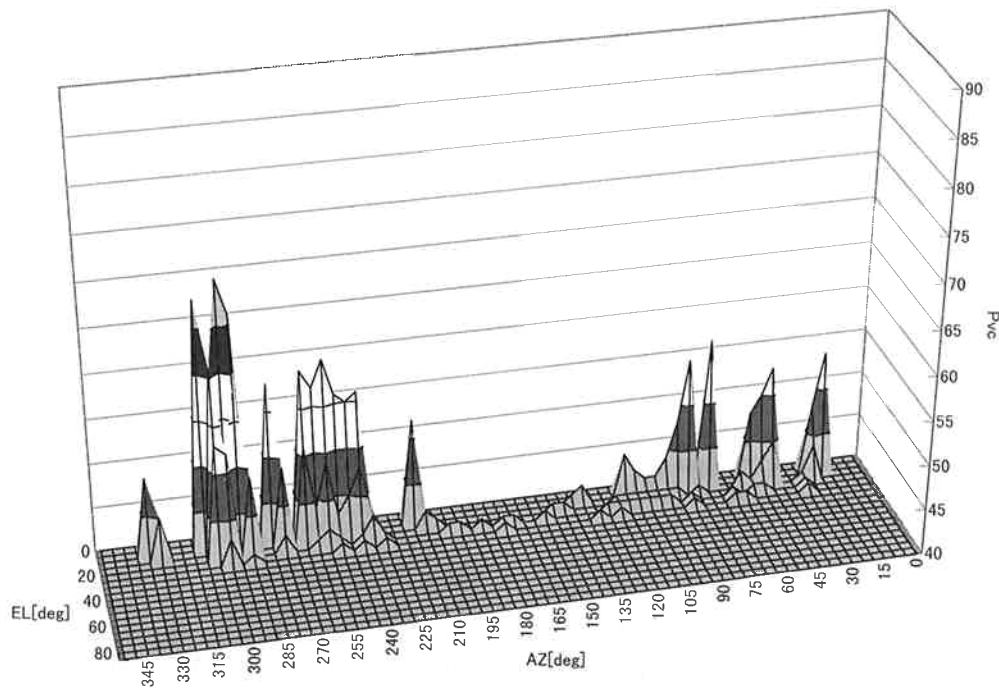
Fig. 2   Result of interference surveying made at Koganei (10ch USB, Aug. 22/1998). Pvc is the readout of video-convertor-monitor.

made at Koganei on video channels 2 and 10 in an X (8 GHz) band. Readouts greater than zenith sky level of a video-converter-monitor are plotted on the azimuth-elevation angle plane. It is clearly shown in the figures that there is a strong interference source at channel 2 in the azimuth direction of 45 degree in a low elevation angle range (<25 degree). In the KSP VLBI system an X band signal is converted into two independent IF signals ranging 500-1000 MHz which correspond to 7700-8200 MHz and 8100-8600 MHz RF signals. We measured the spectrum of both IF signals by using a spectrum analyzer. It was then confirmed that the interference signals actually existed at radio frequencies corresponding to channel 2. Furthermore, since the appearance of interference signals is restricted to certain azimuth ranges and elevation angles, it could be concluded that interferences came from outside RF signals rather than IF signals. If this interference appears every day, we should change the frequency arrangement for routine observation.

3. Output Level Calibration of Video Converter and System Noise

System noise temperature, T_{sys}, is obtained, using a Y factor that is defined as the power ratio between a noise source that is turned on and off, as

$$T_{sys} = T_{ND}/(Y-1) , \quad \cdots\cdots\cdots\cdots\cdots\cdots\cdots(1)$$

where, T_{ND} is an effective temperature of a noise source (noise diode).

The readout of the output level monitor can vary by unit and by channel, and can not be directly used for the calculation of the Y factor. Therefore we have carried

out calibration measurements at each KSP station as follows. We obtained a readout of the output-level-monitor of the video converter at several elevation angles ranging from 90 to 5 degrees. At each elevation angle the noise diode is repeatedly turned on and off. A precise measurement of the video-signal-monitor output level is performed simultaneously by using a power meter (HP437B). As the background sky noise level is changed according to the changes in the elevation angle, we can obtain many combinations of readouts of video-converter-monitor and a power meter measurements at different background sky levels. Thus we can obtain an empirical equation that converts a readout into actual signal power. The equation is:

$$P_{PM} = a(P_{VC})^2 + b(P_{VC}) + c, \quad \cdots\cdots\cdots\cdots\cdots\cdots(2)$$

where P_{PM}, P_{VC} are the readouts of a power meter and video-converter-monitor. The parameters, a, b, and c, which are determined by calibration measurements are summarized in Table 1.

4. Signal Blocking at Each Station

The readout of the video-converter-output monitor can also be used to investigate signal blocking at each station. If there are trees in the line-of-sight from the antenna, this will increase the system noise level. Since this increase does not greatly depend on frequency, it can be easily discriminated from the interference signals as mentioned in section 2.

Figs. 3-6 show the results of the blocking measurements. Calibrated readouts of the X band video-converter-output monitor normalized in the zenith

Table 1a   Parameters of the empirical equation for Koganei

Applicable Range

ch	Band	for Pvc	a	b	c
1	USB	27.-49.	1.901E-01	-2.956E+00	8.265E+01
2	USB	26.-52.	1.469E-01	8.155E-01	8.004E+00
3	USB	30.-59.	1.474E-01	2.497E-01	2.369E+01
4	USB	33.-62.	1.950E-01	-4.100E+00	1.038E+02
5	USB	30.-58.	1.678E-01	-1.699E+00	5.694E+01
6	USB	51.-90.	3.330E-01	-2.189E+01	6.625E+02
7	USB	51.-90.	3.158E-01	-2.102E+01	6.225E+02
8	USB	44.-81.	2.202E-01	-7.825E+00	2.278E+02
9	USB	42.-79.	1.849E-01	-4.663E+00	1.421E+02
10	USB	38.-72.	1.788E-01	-3.411E+00	1.054E+02
11	LSB	55.-94.	3.264E-01	-2.348E+01	7.489E+02
12	LSB	49.-82.	2.396E-01	-1.213E+01	3.708E+02
13	LSB	50.-80.	1.906E-01	-4.803E+00	1.300E+02
14	LSB	57.-92.	6.255E-01	-6.097E+01	1.907E+03
15	LSB	55.-96.	3.251E-01	-2.332E+01	7.317E+02
16	LSB	56.-97.	3.328E-01	-2.487E+01	8.159E+02

Table 1b   Parameters of the empirical equation for Kashima

Applicable Range

ch	Band	for Pvc	a	b	c
1	USB	30.-63.	1.773E-01	-2.847E+00	8.326E+01
2	USB	31.-71.	1.159E-01	2.785E+00	-3.665E+01
3	USB	23.-51.	1.317E-01	1.051E+00	5.265E+00
4	USB	33.-69.	1.710E-01	-2.377E+00	7.141E+01
5	USB	30.-60.	1.714E-01	-1.925E+00	6.117E+01
6	USB	53.-82.	2.528E-01	-1.307E+01	4.280E+02
7	USB	58.-85.	3.499E-01	-2.592E+01	8.654E+02
8	USB	57.-85.	2.158E-01	-7.515E+00	2.357E+02
9	USB	51.-77.	2.384E-01	-1.090E+01	3.555E+02
10	USB	49.-72.	1.997E-01	-5.089E+00	1.746E+02
11	LSB	34.-67.	1.692E-01	-2.391E+00	8.474E+01
12	LSB	27.-56.	1.364E-01	7.097E-01	1.606E+01
13	LSB	32.-67.	1.743E-01	-2.602E+00	8.218E+01
14	LSB	26.-58.	1.580E-01	-8.556E-01	3.992E+01
15	LSB	29.-59.	1.684E-01	-1.764E+00	6.032E+01
16	LSB	37.-76.	2.331E-01	-8.750E+00	2.328E+02

Table 1c Parameters of the empirical equation for Miura

ch	Band	Applicable Range for Pvc	a	b	c
1	USB	44.-70.	1.599E-01	-3.054E−01	5.773E+00
2	USB	45.-70.	2.194E-01	-7.747E+00	2.072E+02
3	USB	44.-69.	1.818E-01	-2.574E+00	6.126E+01
4	USB	42.-68.	1.846E-01	-4.220E+00	1.265E+02
5	USB	46.-74.	1.837E-01	-3.248E+00	8.859E+01
6	USB	48.-77.	1.805E-01	-2.781E+00	7.267E+01
7	USB	49.-83.	2.130E-01	-7.418E+00	2.240E+02
8	USB	42.-71.	2.272E-01	-7.610E+00	1.914E+02
9	USB	25.-47.	9.448E-02	3.815E+01	-3.946E+01
10	USB	26.-47.	8.999E-02	3.978E+00	-4.956E+01
11	LSB	32.-60.	1.403E-01	9.836E−01	-4.213E+00
12	LSB	26.-52.	1.330E-01	7.240E−01	1.225E+01
13	LSB	29.-56.	1.800E-01	-2.770E+00	7.399E+01
14	LSB	29.-56.	1.199E-01	1.621E+00	-9.438E+00
15	LSB	47.-78.	7.458E-02	1.052E+01	-2.763E+02
16	LSB	36.-66.	1.522E-01	-1.045E+00	4.278E+01

Table 1d Parameters of the empirical equation for Tateyama

| ch	Band	Applicable Range for Pvc	a	b	c
1	USB	21.-38.	6.089E-01	-6.508E+00	1.181E+02
2	USB	21.-39.	6.843E-01	-1.094E+01	1.691E+02
3	USB	19.-36.	6.858E-01	-1.085E+01	1.620E+02
4	USB	21.-39.	6.545E-01	-7.648E+00	1.066E+02
5	USB	22.-40.	5.732E-01	-4.857E+00	9.527E+01
6	USB	15.-30.	5.379E-01	-2.919E+00	4.412E+01
7	USB	16.-33.	6.165E-01	-5.282E+00	7.742E+01
8	USB	16.-34.	5.751E-01	-5.275E+00	8.101E+01
9	USB	15.-32.	5.975E-01	-4.882E+00	7.019E+01
10	USB	16.-31.	6.433E-01	-6.877E+00	8.943E+01
11	LSB	23.-46.	1.040E-01	1.037E+00	-2.461E+00
12	LSB	20.-45.	1.491E-01	3.124E−01	5.817E+00
13	LSB	23.-48.	1.058E-01	2.406E+00	-1.709E+01
14	LSB	25.-52.	1.711E-01	-5.665E−01	2.775E+01
15	LSB	22.-45.	1.256E-01	1.273E+00	-1.003E+00
16	LSB	27.-53.	1.741E-01	-2.109E+00	6.271E+01
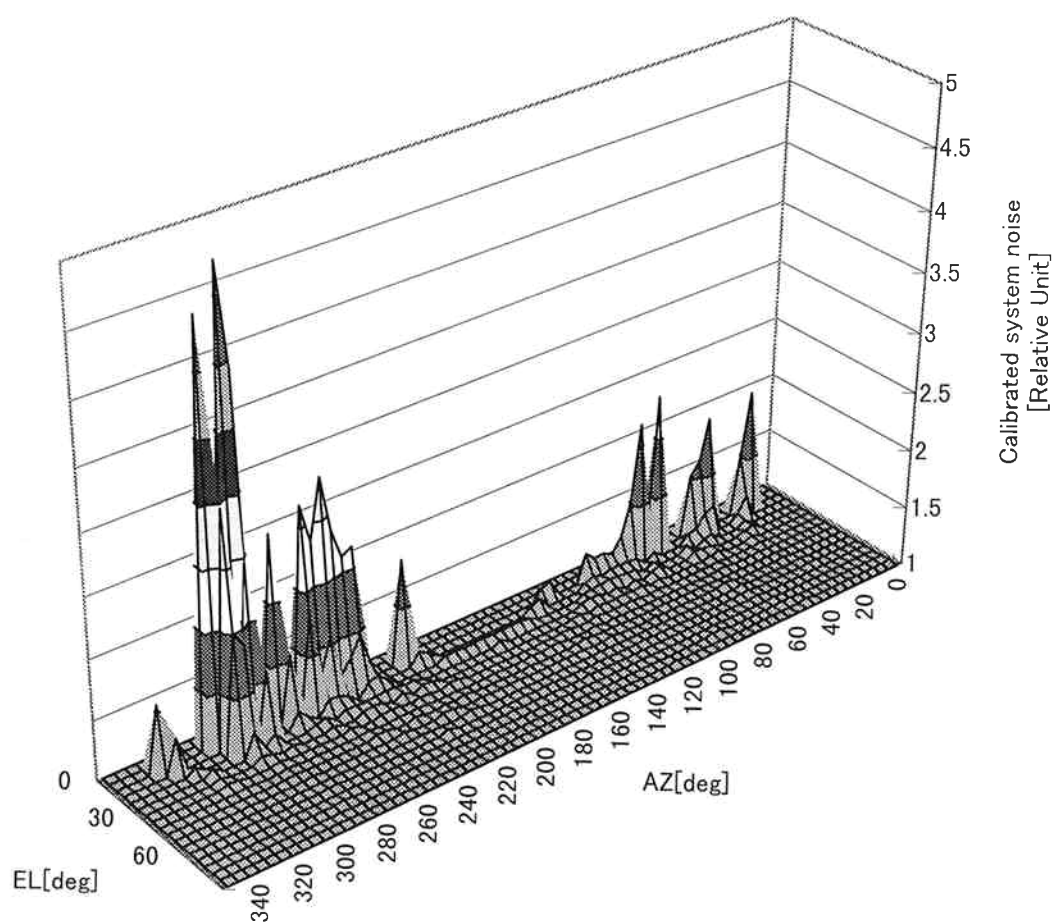
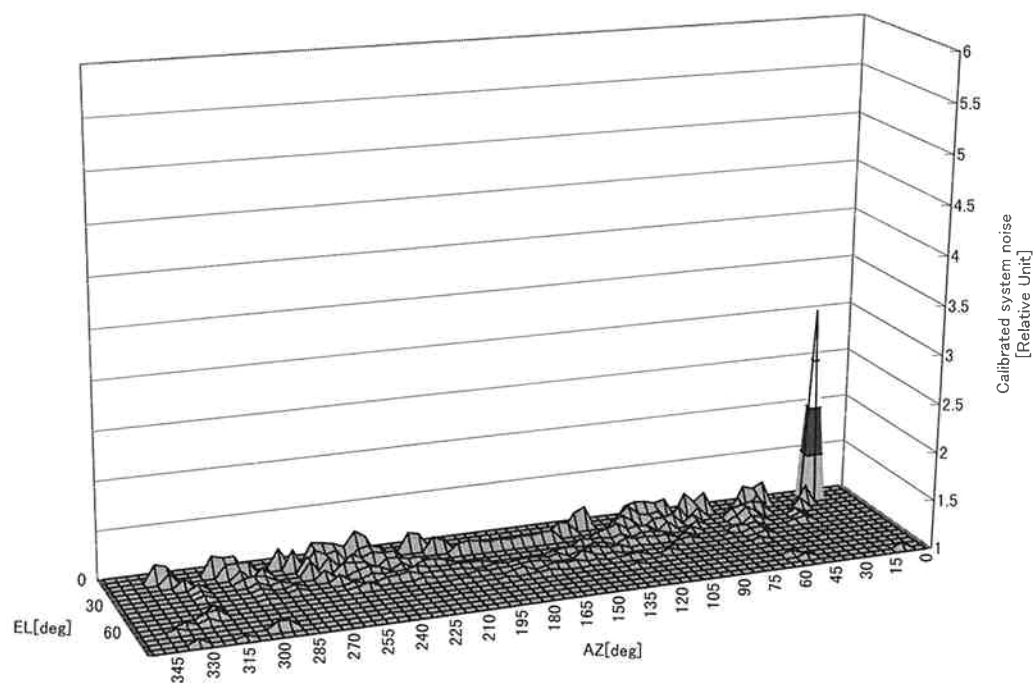**Fig. 3 Result of blocking measurements. (Koganei, X band)**

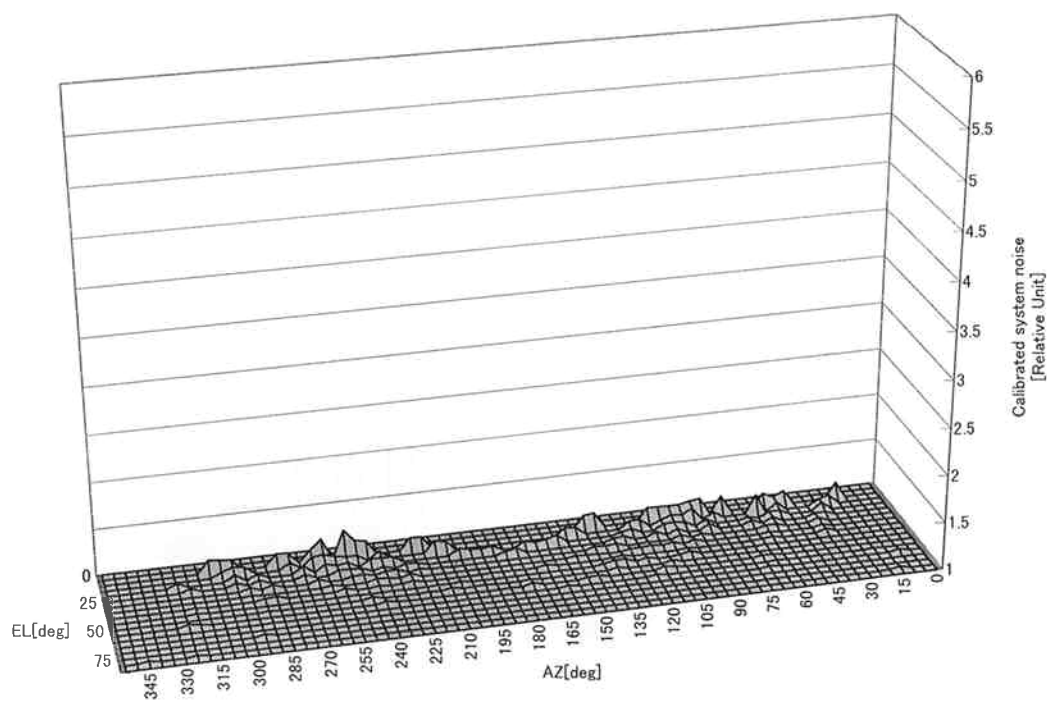**Fig. 4 Result of blocking measurements. (Kashima, X band)**

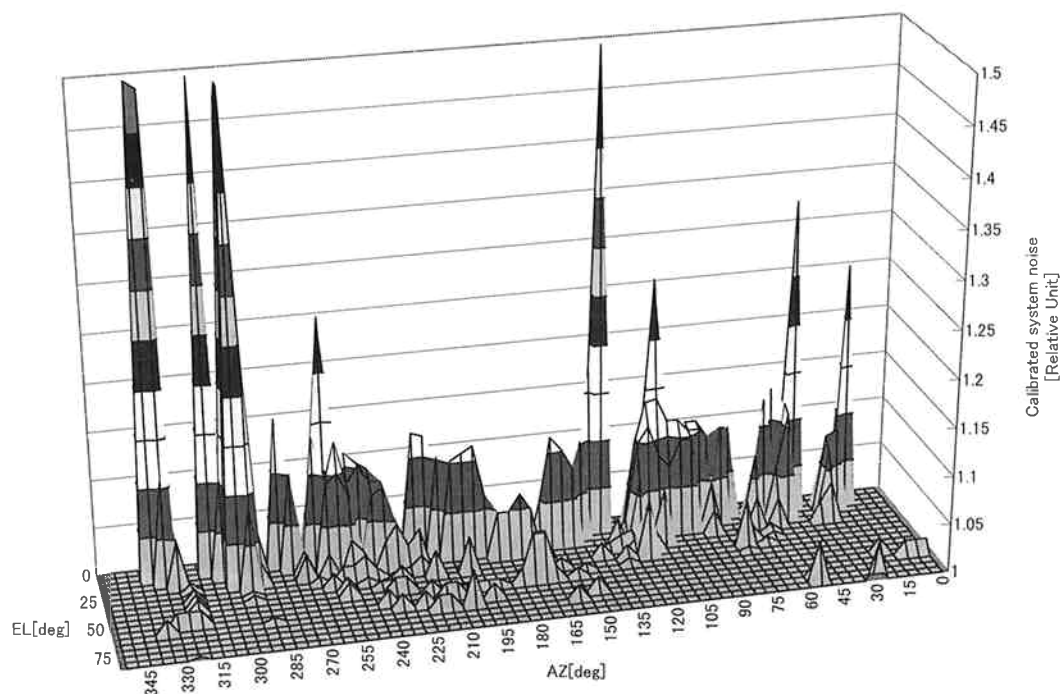Fig. 5 Result of blocking measurements. (Miura, X band)

Fig. 6 Result of blocking measurements. (Tateyama, X band)

direction and are plotted on the azimuth-elevation angle plane. Calibrated readouts except for those channels that have interference are averaged over the video channels in the X band.

5. Evaluation of Correlation Amplitude

In a geodetic VLBI, the time delay of signals received at two different stations is measured by using a cross-correlation technique, i.e., the time delay is obtained as a trial time shift that maximizes cross correlation amplitude. And many delay times that are obtained in an experiment are used for baseline analysis that estimates mainly the position of stations. Radio sources observed by VLBI are usually very weak, so that most of the received signals contain noise. Therefore in general cases correlation amplitude, ρ, becomes very low. It is calculated as,

$$\rho = [\{T_{star1}/(T_{system1}+T_{star1})\}$$
$$\cdot \{T_{star2}/(T_{system2}+T_{star2})\}]^{1/2}, \quad \cdots\cdots\cdots\cdots (3)$$

where, T_{star} is the increase of noise temperature due to the radio source, T_{system} is system noise temperature, and suffixes 1 and 2 denote stations. T_{star} is given by

$$T_{star} = SLA\eta/k, \quad \cdots\cdots\cdots\cdots\cdots\cdots\cdots\cdots (4)$$

where, S, L, A, η, and k denote correlated flux, attenuation due to propagating medium, antenna aperture area, aperture efficient, and Bolzmann's constant. In the KSP VLBI system, all antennas have the same size and almost the same performance. So that T_{star1} and T_{star2} are supposed to be the same amount (T_{star}). Moreover T_{star} is very weak compared with the system noise. Hence we can re-write eq. (1) as,

$$\rho = T_{star}\{1/T_{system1}\cdot T_{system2})\}^{1/2}$$
$$= SLA\eta\{1/(T_{system1}\cdot T_{system2})\}^{1/2}k. \quad \cdots\cdots\cdots\cdots (5)$$

By calibrating the system to measure T_{system}, it is possible to obtain $S\,L$, which includes attenuation due to a propagating medium, as

$$SL = \{\rho k(T_{system1}\cdot T_{system2})\}^{1/2}/A\eta. \quad \cdots\cdots\cdots\cdots (6)$$

Examples of $S\,L$ obtained for radio source 4C39.25 observed on June 13, 1998 on the Kashima-Tateyama baseline are shown as a function of elevation angle in Fig. 7 for an X band and in Fig. 9 for an S band. As for the same observations, correlation amplitudes are shown in Figs. 8 and 10. We can see a large variation in the correlation amplitude because it was a rainy day. However the $S\,L$ shows a less variation compared with the correlation amplitude. This demonstrates that the measurement of correlation amplitude can be improved by applying the correction of system noise. This correction works well for observations made under bad weather conditions such as rain.

6. Conclusion

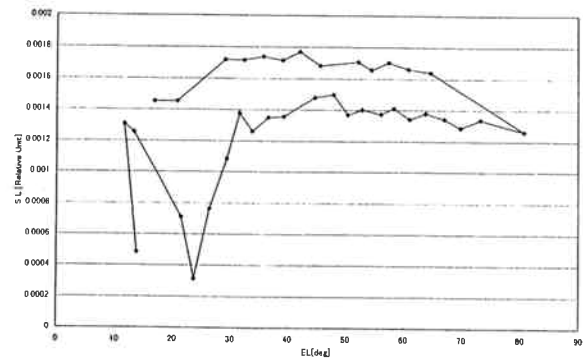The KSP video converter has the function of video-signal-level monitoring. This function is used not only for

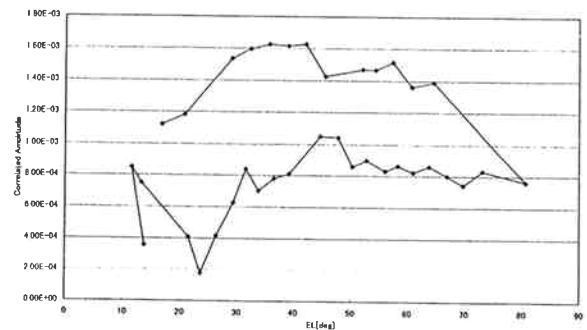Fig. 7 S L at X band (Kashima-Tateyama, 4C39.25, Jun. 13/1998)

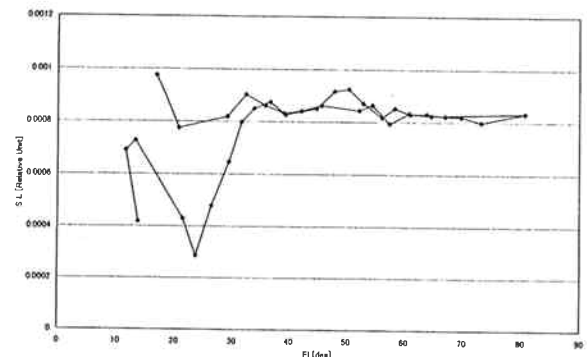Fig. 8 Correlated amplitude at X band (Kashima-Tateyama, 4C39.25, Jun. 13/1998)

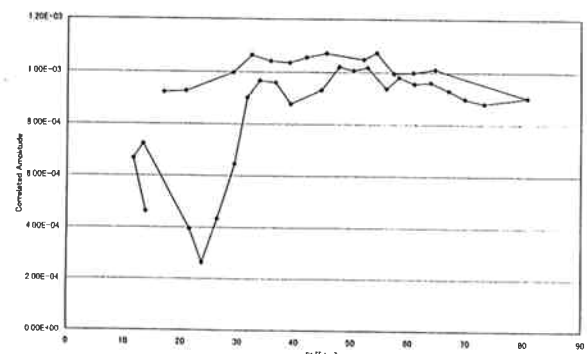Fig. 9 S L at X band (Kashima-Tateyama, 4C39.25, Jun. 13/1998)

Fig. 10 Correlated amplitude at X band (Kashima-Tateyama, 4C39.25, Jun. 13/1998)

the adjustment of video out signal levels in order to
match a suitable level for the input interface unit but
also for monitoring the occurrence of interferences and
surveying signal blocking. Moreover it can be applied to
calibrating the correlation amplitude in order to obtain
reliable observations that are necessary for investigating
long term variations of source amplitude. We are also
planning to utilize this data to evaluate how seasons af-
fect the observed correlation amplitude.

References

(1) A. E. E. Rogers, "Very Long Baseline Interferometry
     with effective band width for phase-delay measure-
     ment", Radio Science Proc, vol. 5, no. 10, pp. 1239-
     1247, Oct. 1970.
(2) H. Kiuchi, et al., "K-4 VLBI Data-Acquisition sys-
     tem", Publ. Of Astron. Soc. of Japan, vol. 49, no. 6,
     1997.

Kouichi SEBATA
Keystone Project Team
VLBI
E-mail: seba@crl.go.jp

Jun AMAGAI
Keystone Project Team
Hardware development for radio inter-
ferometer and satellite laser ranging
E-mail: amagai@crl.go.jp

Tetsuro KONDO
Kashima Space Research Center
Space geodesy
E-mail: kondo@crl.go.jp

Noriyuki KURIHARA
Radio   Astronomy   Application
Section
Kashima Space Research Center
VLBI, Space geodesy
E-mail: kurihara@crl.go.jp